



## Visualization of hydrogen distribution around blisters by tritium radio-luminography

T. Hoshihira \*, T. Otsuka, T. Tanabe

*Interdisciplinary Graduate School of Engineering Sciences, Kyushu University, 6-1, Kasuga-kouen, Kasuga, Fukuoka, Japan*

### A B S T R A C T

Hydrogen distribution around blisters on aluminum (Al) and molybdenum (Mo) was examined by tritium radio-luminography, i.e. tritium autoradiography (TARG) and an imaging plate technique. Tritium accumulated in the blisters on Al surface was successfully visualized at the first time. The tritium density in the blisters was found to increase with their radius to the power of 2.3. This supports the blister mechanism of bubble coalescence but the blister shape was flattened along the surface with increasing their size. For Mo, tritium distribution was not well correlated with blisters, and the bubbles coalescence was not clearly observed, too. But the erosion or exfoliation of thick layers with wider area than blisters were observed and hydrogen was released by the exfoliation of the thick surface layers, remaining not tritium on the exfoliated surface. Such exfoliation is very likely caused by mechanical stress given by accumulated hydrogen at trapping site such as grain boundaries, intrinsic defect, or self trapping.

© 2009 Elsevier B.V. All rights reserved.

### 1. Introduction

It is well known that energetic hydrogen ion irradiation results in blistering and/or grains exfoliations of materials surface. Different from inert gas ions like helium (He), neon (Ne) and argon (Ar), hydrogen (H) easily diffuses into materials and some times makes strong interactions with target atoms. Hence mechanism of hydrogen blistering could be somewhat different from those given by the inert gas ions. Although extensive works have been done, the mechanism of hydrogen blistering is still unclear; particularly the role of hydrogen is not well understood.

At least two different types of hydrogen blistering have been observed, one appearing well above DBTT, like Al [1] and nickel (Ni) [2] and the other appearing near and below DBTT, like Mo [3] and tungsten (W) [4]. Hydrogen solubility and diffusivity is very small for both metals. In case of Al, typical blister structure with spherical form appears on surface and the thickness of blister skins is nearly equals to the projected range or the peak damaged position. In Mo and W, non-spherical and the exfoliation of thicker layers than projected range were often observed.

To understand such different blistering appearances, it is critically important to understand hydrogen behavior. This motivated us to apply a tritium tracer technique, tritium radio-luminography, to observe hydrogen (tritium) behavior on blistering. Firstly, we injected hydrogen gas including tritium in materials to make blisters. Then tritium areal distribution was determined by the tritium radio-luminography, either tritium autoradiography (TARG) or a

tritium imaging plate (TIP) technique, to observe hydrogen distribution and/or accumulation in blisters and surrounding area.

TARG has been utilized to show hydrogen accumulation in steels [5–7] detecting  $\beta$ -electrons emitted from tritium by a photographic emulsion film formed on samples surface. This is the same technique to make photograph which uses optical photons instead of the  $\beta$ -electrons.

The TIP technique uses photo stimulated luminescence (PSL) phenomenon, instead of the photographic technique and has been successfully applied to determine areal distribution of tritium on the plasma-facing surface of various plasma devices [8–10]. The tritium distribution is record as the number and position of color centers formed in photogenic crystals. After the exposure, the excitation of the color centers by a laser beam produces PSL, scanning the laser beam; one can get areal distribution of PSL intensity on the surface corresponding tritium profiles.

### 2. Experimental

Specimens used here were Mo and Al rectangular sheets of  $5 \times 5 \text{ mm}^2$  with the thickness of 1 mm. The surface of the specimens was mechanically polished with abrasive papers and finished with  $0.3 \mu\text{m Al}_2\text{O}_3$  powders. Two different hydrogen loading methods were used; one is electrochemical charging and the other is AC glow charging.

For Al case, the electrochemical charge method was used with tritiated NaOH aqueous solution with T concentration of  $1.5 \times 10^{-5}$  in T/H ratio. A Pt anode plate was arranged parallel to the cathode specimen and the loading was made with a current density of  $10 \text{ A/m}^2$  at RT for 5 – 10 min to produce blisters. For

\* Corresponding author. Tel./fax: +81 92 642 3795.

E-mail address: [hoshi@aees.kyushu-u.ac.jp](mailto:hoshi@aees.kyushu-u.ac.jp) (T. Hoshihira).

Mo case, tritium was loaded by the AC glow discharge method with  $H_2$  gas of 27 Pa containing T with  $5 \times 10^{-6}$  in T/H ratio. Mo specimens were fixed to an electrode and covered by a stainless plate with a hole of 3 mm in diameter. AC voltage of 3 keV was applied between the two electrodes to make AC glow discharge and only selected areas of the specimens with 3 mm in diameter were exposed to the discharge for long time to get surface blisters and their exfoliation. The irradiated surfaces of the specimens were observed by an optical microscope and a scanning electron microscope (SEM).

TARG was done as follows. Two layers, a collodion film with 20 nm and a layer of nuclear photographic emulsion of AgBr grains (Amersham EM-1), were coated and dried on the tritiated specimen surface with dipping method in a photo-dark room. The former was placed between the specimen surface and the nuclear emulsion in order to avoid any chemical reactions of AgBr with the specimen metal. The photographic film thus produced was exposed to tritium  $\beta$ -electrons which have an average energy of 5.7 keV escaping from the specimen surface for about 10 days in a shielded box at liquid nitrogen temperature to avoid T migration and release during the exposure. After the exposure, the photographic film was developed and fixed to get Ag precipitates with about 0.3  $\mu\text{m}$  in diameter. The profile of Ag precipitation was observed by SEM and energy dispersive X-ray spectroscopy (EDS), correspond tritium profile on the sample.

In the case of Mo, tritium distribution was examined by TIP which has higher sensitivity than TARG. The T loaded surface of the specimen was exposed to an imaging plate (IP: FUJIFILM BAS-TRI2025) at liquid nitrogen temperature for 24 h. Then, IP was processed by an IP reader (FILMFILM BAS2500) to get areal intensity profiles of PSL which correspond to areal tritium retention profiles.

### 3. Results

#### 3.1. Al

Fig. 1(a) is an optical microscope image of blisters formed on Al specimen surface. The blisters with various radius of 1–5  $\mu\text{m}$  were distributed rather homogeneously. And some blisters coalesced to make larger non-spherical blisters. Fig. 1(b) is a result of TARG on Al surface obtained by SEM and EDS. In the SEM image, blister shapes are more clearly observed and silver precipitates appeared as accumulated white dots on the blister surface representing T distribution. In our knowledge, this is the first clear observation (TARG) of hydrogen (tritium) accumulation in the blisters. One can note that the silver precipitates on the non-blistered area are very seldom. This indicates that hydrogen concentration in blisters is much higher than that in the non-blistered area.

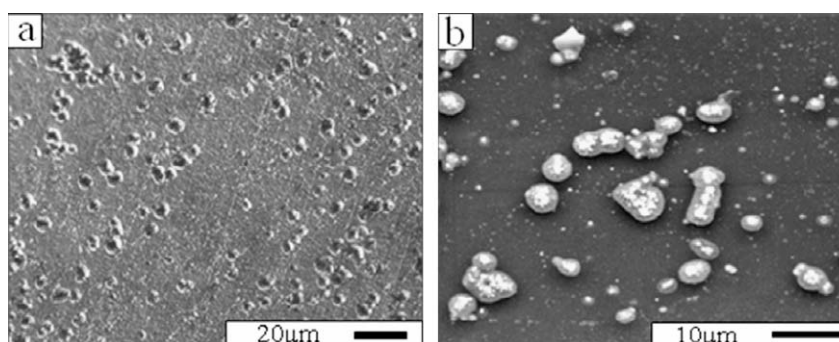


Fig. 1. (a) Blisters formed on Al surface obtained by an optical microscope after tritium loading and (b) TARG given as a SEM image of blisters with silver precipitates on the Al surface.

#### 3.2. Mo

Fig. 2(a) is an optical microscope image of the hydrogen loaded Mo surface by the AC glow discharge. One can distinguish three different surface appearances, heavily damaged and less damaged regions and boundary regions between the former two, respectively shown in Fig. 2(a), (b) and (c). It is noted that the tritium distribution determined by IP (Fig. 2(d)) is well correlated to the surface appearances. The heavily damaged region located at the central area (Fig. 2(a)) was significantly eroded and very rough, remaining lots of traces of blister flaking and exfoliation of local surface-areas (referred as eroded region hereafter). Clear blistering was appeared on the less damaged region at the outer area (Fig. 2(b), referred as blistered region hereafter). Between the eroded region and the blistered one, there appeared clear height difference to give the overall erosion thickness of more than 1  $\mu\text{m}$ , far deeper than the hydrogen implanted depth. In the blistered region, many small blisters with a diameter of about 1  $\mu\text{m}$  were formed but the areal blister density was quite inhomogeneous with clear distinction between smooth area and blistered area, which is very likely caused by different orientations of grains.

Fig. 2(e) is a line profile of tritium along the dashed line in Fig. 2(d). The tritium intensity for the blistered region was three times higher than that of the erode region. One can note that the tritium intensity in the blistered region was quite uniform without any indication of tritium accumulation in the blister as observed in Al. Compared to the blistered region, tritium intensity was clearly scattered at the eroded area. One note that tritium distribution well corresponds to the local exfoliation of the surface layers or blister flaking with less tritium in the exfoliated area. The tritium release caused by the exfoliation or flaking was appreciable in the IP image of the transition region between the eroded and the blistered regions.

We have also made TARG of those surfaces particularly for blistered area. However no clear T localization on blister surfaces such as appeared Al blisters was observed. One main reason would be T concentration was not high enough to make clear TARG image (IP is much sensitive than TARG). Another possible reason is smaller penetration length of the  $\beta$ -electrons of T in Mo than that in Al, which is discussed in the next section.

### 4. Discussions

#### 4.1. Analyzing depth of tritium by TARG and TIP

Since the average energy of  $\beta$ -electrons emitted from T, 5.7 keV, is rather low, TARG and TIP can detect tritium retaining within a certain depth from the surface, referred as an escaping depth. The escaping depth depends on electron stopping power and can

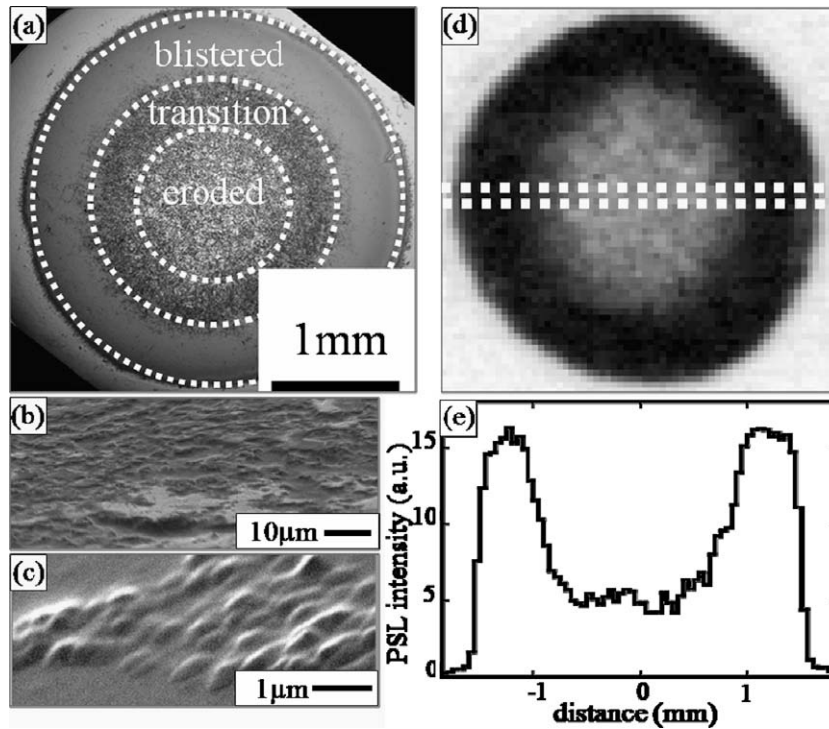


**Fig. 2.** (a) Surface images obtained by an optical microscope, (b) a SEM image for eroded area, (c) a SEM image for blistered area, (d) the IP image corresponding to (a) and (e) the tritium profile along dashed line in (d) for heavily hydrogen loaded Mo.

be calculated by a simulation code. Applying the MCNP code [11], one of the most often used, the escaping depths of 5.7 keV for Al and Mo were calculated as shown in Fig. 3. One can see that TARG and IP can detect tritium retained within 0.5  $\mu\text{m}$  from the surface for Al, while only 0.2  $\mu\text{m}$  for Mo. This indicates that TARG and IP can detect tritium behind blister skins in Al, while that in Mo seems difficult. This could be one of the reasons for the difficulty to get clear TARG corresponding the blistering for Mo.

For Al, according to the escaping depth of  $\beta$ -electron, the thickness of blister skins were considered to be less than 0.5  $\mu\text{m}$  and there were few tritium gas bubbles at the other area at least

0.5  $\mu\text{m}$  in depth from the surface. In brief, hydrogen gas was accumulated into blisters remaining less hydrogen in the matrix as discussed below.

#### 4.2. Tritium accumulated in blisters

As discussed above, TARG for Al can detect all T in the blisters as well as those retained within  $\sim 0.5 \mu\text{m}$  which is much deeper than the implanted depth of T. With using a particle analysis software package [12], radius of blisters and Ag precipitates were determined. In Fig. 4 are plotted the local Ag densities on the blisters against the blister radius in a logarithmic scale. Here we can

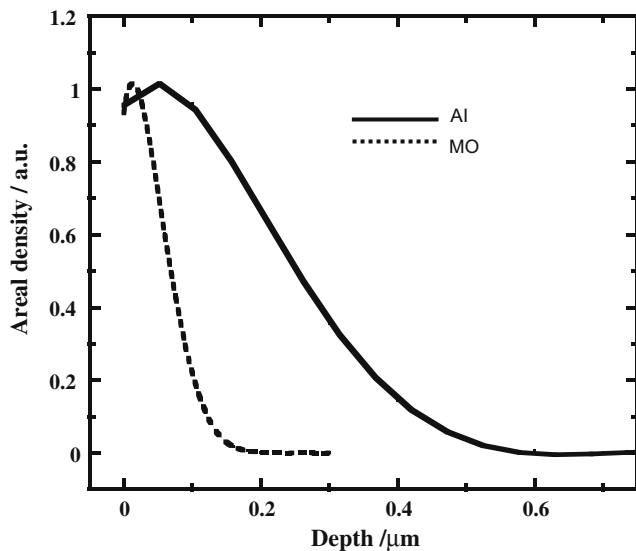


**Fig. 3.** Penetration depth of  $\beta$ -electrons with incident energy of 5.7 keV in Al and Mo calculated by the MCNP code.

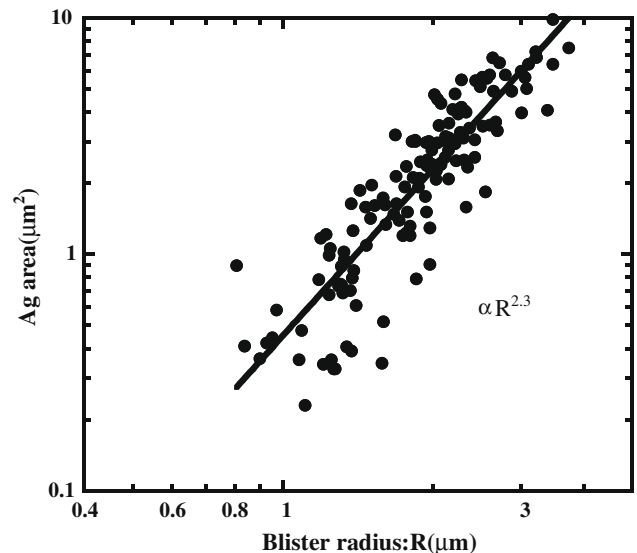


**Fig. 4.** The relation between blister radius and Ag precipitates on the Al surface.

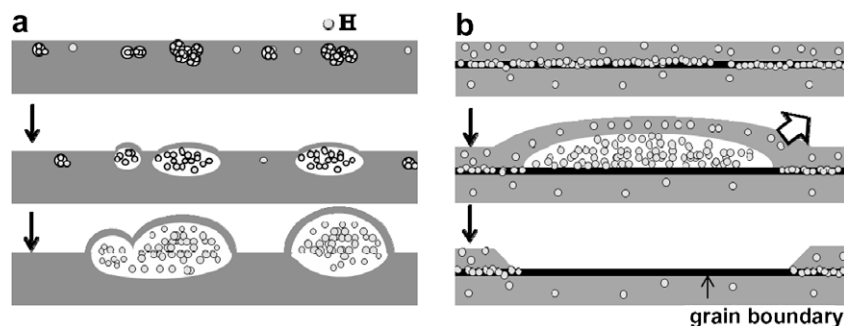


Fig. 5. Schematic views for the blistering processes for (a) Al and (b) Mo.

assume Ag density is proportional to the integrated decay number of T or number density of the emitted electrons, which is confirmed by a standard sample technique. Although the data are widely scattered, there is a clear correlation between the tritium densities and the blister radius and the former increase with the latter to the power of 2.3, but not square nor cube.

According a simple theory [13], gas pressure,  $P$ , in a bubble with a radius  $R$  is equilibrated with the surface tension,  $\gamma$ , of the bubble:

$$\frac{2\gamma}{R} = P \quad (1)$$

If bubbles coalesce with each other to grow larger one, the volume of a newly created bubble which has a volume  $V$  with a diameter  $R$ , keeping constant  $\gamma$  or constant  $P$ , the amount of tritium should increase with  $R$  square, different from the observation of  $R^{2.3}$ .

This means the blister shape is neither spherical nor hemispherical. In other words, gas pressure in the Al blisters was not constant or did not keep the Eq. (1). Since bubbles created in the subsurface layers must be spherical, the bubble growth mechanism is not a simple bubble coalescence to make a larger spherical bubble. It is most likely that the coalescence results in the bubble flattening with additional opening at the edge owing to cleavage due to the stress accumulation. Still we need further analysis to explain  $R^{2.3}$  dependence quantitatively.

#### 4.3. Mechanism of blistering/flaking

Considering all results, we schematically draw blistering process for Al and Mo in Fig. 5(a) and (b), respectively. In Al, owing to its high ductility and very small diffusivity and solubility of hydrogen, implanted hydrogen easily accumulates to make small bubbles remaining quite less tritium in the matrix. Then the bubbles coalesce to grow. The growth continues attracting neighboring small bubbles and make blisters at the surface. The shape of the blisters is not likely spherical nor hemispherical and hydrogen pressure (tritium density) decreases with increasing the blister size. The bubble growth could be also assisted by stress accumulation at the edge of the non-spherical blister shape as discussed above. In case if the plastic deformation during the blister growth could sweep the tiny bubbles, the matrix would retain less T.

In the case of Mo, hydrogen is not likely to accumulate to bubbles beneath the surface but accumulate at grain boundaries and/or other hydrogen trapping sites much deeper than the escaping depth of the  $\beta$ -electrons of T. Such local hydrogen accumulation results in the exfoliation of the rather thick local layers owing to plastic deformation when stress given by the accumulated hydrogen exceeds the yield stress of Mo. As a result, no tritium

was remained at the exfoliated area. Still as already discussed, T in Mo blisters could not be detected by TARG, because the thickness of the blister skins of Mo is very likely over the penetration depth. To confirm this TARG with using more intense T is needed.

#### 5. Conclusion

We have successfully applied tritium radio-luminography to examine hydrogen blistering mechanisms. In our knowledge, TARG (Fig. 1(b)) which clearly shows tritium accumulation in the Al bubbles is the first successful result and proved to be very useful to examine hydrogen blistering mechanism. The results are summarized as follows.

For Al, tritium was accumulated in blisters remaining little tritium in the matrix. This is a clear indication that bubbles grew by coalescence each. The tritium density in a bubble of radius  $R$  increased with the power of 2.3, indicating blister flattening.

For Mo, bubbles coalescence was not observed and hydrogen was released by exfoliation of thick surface layers. After the exfoliation no tritium was retained. This indicates that blistering is caused by plastic deformation owing to mechanical stress given by accumulated hydrogen at trapping sites such as grain boundaries, intrinsic defect, or self trapping.

In this study, we have employed two different hydrogen loading methods, which significantly differ the loading hydrogen flux. There could be some effect of the loading flux on blistering and fracturing, which are now under examination.

#### References

- [1] R. Checchetto, L.M. Gratton, A. Miotello, Surf. Coat. Technol. 158 (2002) 356.
- [2] E. Abramov, San-Qiang Shi, D.A. Thompson, W.W. Smeltzer, J. Nucl. Mater. 186 (1991) 61.
- [3] Tatsuo Sugie, Satoshi Kasai, Masaki Taniguchi, Masaaki Nagatsu, Takeo Nishitani, J. Nucl. Mater. 329&333 (2004) 1481.
- [4] Y. Ueda, T. Funabiki, T. Shimada, K. Fukumoto, H. Kurishita, M. Nishikawa, J. Nucl. Mater. 337 (2005) 1010.
- [5] M. Garet, A. M. Brass, C. Haut, F. Guttierrez-Solana, Corros. Sci. 40 (7) 1073.
- [6] H. Hitoshi, T. Otuska, H. Nakashima, S. Sasaki, M. HAYakawa, M. Sugisaki, Scr. Mater. 53 (2005) 1279.
- [7] G. Katano, K. Ueyama, M. Mori, J. Nucl. Mater. 36 (9) 2277.
- [8] K. Miyasaka, T. Tanabe, G. Mank, K.H. Finken, V. Philipps, D.S. Walsh, K. Nishizawa, T. Saze, J. Nucl. Mater. 290 (2001) 448.
- [9] K. Sugiyama, K. Miyasaka, T. Tanabe, M. Glugla, N. Bekris, P. Coad, J. Nucl. Mater. 313 (2003) 507.
- [10] T. Tanabe, K. Miyasaka, K. Masaki, K. Kodama, N. Miya, J. Nucl. Mater. 307 (2002) 1441.
- [11] J. F. Briesmeister, Los Alamos National Laboratory Report LA-12625-M, 1993.
- [12] W. S. Rasband, Image J. Bethesda, US National Institutes of Health, <<http://rsb.info.nih.gov/ij/>>.
- [13] S. Muto, T. Matsui, T. Tanabe, J. Nucl. Mater. 290 (2001) 131.